

## Excited-State Backbone Twisting of Polyfluorene As Detected from Photothermal After-Effects

H. L. Chen,<sup>†</sup> Y. F. Huang,<sup>‡</sup> T. S. Lim,<sup>‡</sup> C. H. Su,<sup>§</sup> P. H. Chen,<sup>||</sup> A. C. Su,<sup>\*,||</sup> K. T. Wong,<sup>⊥</sup> T. C. Chao,<sup>⊥</sup> S. I. Chan,<sup>#</sup> and W. Fann<sup>†,‡</sup>

Department of Physics, National Taiwan University, Taipei 106, Taiwan, Institute of Atomic and Molecular Sciences, Academia Sinica, Taipei 106, Taiwan, National Synchrotron Radiation Research Center, Science Industrial Park, Hsinchu 300, Taiwan, Department of Chemical Engineering, National Tsing Hua University, Hsinchu 300, Taiwan, Department of Chemistry, National Taiwan University, Taipei, 106, Taiwan, and Institutes of Chemistry, Academia Sinica, Taipei 115, Taiwan

Received: February 20, 2009; Revised Manuscript Received: April 22, 2009

By means of time-resolved photoluminescence and photothermal techniques, after-effects from excited-state dynamics, energy migration, and conformational rearrangement of poly(9,9-di-*n*-octyl-2,7-fluorene) (PFO) and its homologues has been examined and interpreted with rotational potential maps from quantum mechanical calculations. Steady-state photoluminescence spectral changes and time-resolved photoluminescence measurements of oligofluorenes and PFO diluted in toluene suggest excited state ring torsion occurring within 30 ps of photoexcitation. With all effects from internal conversion/intersystem crossing processes properly accounted for, we show that the conformational changes associated with this twisting motion can be quantitatively probed by means of photothermal methods. Results suggest mean torsion between neighboring fluorene units by ca. 40° upon excitation, in agreement with the shift of rotational potential minimum from ±40° (and ±140°) in the ground state to ±20° (and ±160°) in the first excited singlet state according to results of quantum mechanical calculations.

### Introduction

Photoinduced torsional motion of macromolecules, such as the photosynthesis process of plants or in the light-sensing function of retina, is of fundamental importance for energy flow in biomolecular systems.<sup>1–3</sup> Similar events are expected for semiconducting polymers, which are nevertheless simpler in structure than their biological counterparts and may serve as model systems for closer scrutiny. This intramolecular torsion may bear significance in donor–acceptor energy transfer,<sup>4</sup> isomerization translation in the excited state,<sup>5</sup> intrachain mobility,<sup>6</sup> and various nonradiative decay processes<sup>7–9</sup> in the photo-physics of conjugated polymer. Based on quantum mechanical calculations and experimental measurements, previous reports showed that large-amplitude torsional motion might induce red-shifted emission spectra in oligomeric systems.<sup>10–17</sup> Such a spectral change has indeed been observed via time-resolved photoluminescence (TRPL) at elevated temperatures and hence decreased solvent viscosity, but the possibility of energy migration via intrachain interactions (which may also result in red-shifted emission) was not excluded.<sup>18,19</sup>

Among conjugated polymers, poly(alkylfluorene)s (PFs) are known to be of high fluorescence quantum yield and good charge mobility; polymers based on the fluorene structure have impacted significantly the development of semiconducting polymers and devices.<sup>20–23</sup> For PFs, TRPL has demonstrated red-shifted spectra in the picosecond time scale.<sup>24</sup> The charac-

teristic time for intramolecular vibrational relaxation in PFs has been obtained as ca. 130 fs.<sup>25</sup> Using different solvents at various temperatures, Dias et al.<sup>26</sup> ruled out the solvent effect from possible causes of the red-shifted emission and estimated a rotational barrier of ca. 0.10 eV.<sup>27</sup> Hintschich et al.<sup>28</sup> further used oligomers and MeLPPP as standards for comparison with emission spectra to distinguish the two effects on the spectral changes in PFs. However, as there were no quantitative methods to directly monitor the conformational relaxation, the exact origin of the conformational changes remained unclear. Here we report observations on the conformational relaxation process of poly(9,9-di-*n*-octyl-2,7-fluorene) (PFO) and its homologues via a combination of picosecond fluorescence spectroscopy with ns-to-μs photothermal techniques of photoacoustic calorimetry (PAC) and photothermal beam deflection (PBD). With all effects from internal conversion and intersystem crossing processes carefully evaluated, we show that the two photothermal techniques (although much delayed in time) yield consistent and complementary information on the excited-state torsion by detecting consequential acoustic and lensing effects.<sup>29</sup>

### Results and Discussion

**Steady-State Absorption/Emission.** Figure 1 gives the steady-state absorption and photoluminescence (PL) spectra of dilute solutions of PFO, corresponding heptamer (F7), pentamer (F5), trimer (F3), and TSBF (chemical structure given as an inset) in toluene. All absorption spectra are of similar full width at half-maximum (ca. 0.49 eV) with maxima located at 3.20, 3.32, 3.37, 3.53, and 3.50 eV, respectively. The clear red-shifts with increasing number of fluorene units indicate increasing conjugation lengths.<sup>30</sup> The emission maximum (0–0) is also red-shifted generally from TSBF/F3 (3.15 eV), F5 (3.02 eV), F7 (2.99 eV), to PFO (2.98 eV), consistent with the increase of conjugation

\* To whom correspondence should be addressed.

<sup>†</sup> Department of Physics, National Taiwan University.

<sup>‡</sup> Institute of Atomic and Molecular Sciences, Academia Sinica.

<sup>§</sup> National Synchrotron Radiation Research Center.

<sup>||</sup> National Tsing Hua University.

<sup>⊥</sup> Department of Chemistry, National Taiwan University.

<sup>#</sup> Institutes of Chemistry, Academia Sinica.

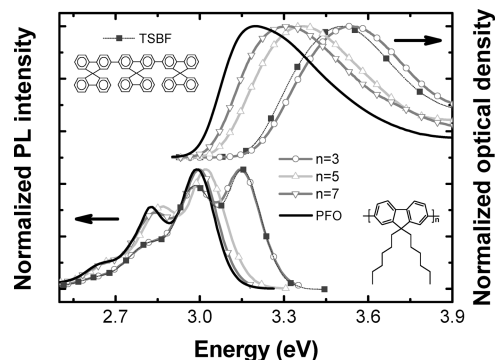


**Figure 1.** Optical absorption and steady-state fluorescence emission spectra of TSBF, F3, F5, F7, and PFO in toluene.

length.<sup>31,32</sup> In particular, emission spectra of F7 and PFO nearly coincide, with the latter very slightly red-shifted by 0.01 eV. This indicates that the effective conjugation of PFO extends not far beyond 7 repeat units. All the PL spectra exhibit clearly identifiable phonon sidebands ca. 0.17 eV (or 1350 cm<sup>-1</sup>) in gap that corresponds to phenylene ring stretching.<sup>33</sup> Furthermore, nearly overlapping absorption and emission spectra of TSBF and F3 (which share the same backbone structure) indicate backbone-dominated dipole transition in the present homologues.

**Time-Resolved Photoluminescence.** Picosecond time-resolved photoluminescence (TRPL) spectra (obtained by use of a streak camera) in Figure 2 demonstrate spectral evolution at different time delays (from 15 to 120 ps) for PFO, F7, F3, and TSBF. Spectral red-shifts (by ca. 0.02 eV) are consistently observed in 0–0 and 0–1 lines. In contrast, TRPL spectra of F3 and TSBF are largely independent of time and are similar to their continuous wave counterparts, indicating that decay processes in PFO and the longer oligofluorenes are similar but distinctively different from those in F3 and TSBF. Moreover, we have made TRPL measurements of PFO in solvents of different viscosities; the results (cf. Figure 2e,f) indicate that the excited-state lifetime of PFO is slightly longer in decalin (2.4 cP) than that in toluene (0.6 cP). We are therefore left with the alternative mechanism of energy migration and conformational change. In addition, the PL amplitude evolution (Figure 2a–d) shows different behavior between TSBF (F3) and PFO (F7) over the time scale. Spectral dynamics of PFO, F7 and F5 are of the similar tendency to that reported by Chang et al.,<sup>34</sup> implying the existence of conformational relaxation.

For isolated chains in dilute solutions, the red-shift may be attributed to intrachain excitonic energy transfer or backbone conformation rearrangement at picosecond time scale.<sup>18</sup> Although energy migration could lead to continuously red-shifted spectra, this mechanism is incommensurate with the limited size of oligomers (significantly shorter than the persistent length of 7 nm for PFO)<sup>35</sup> and hence may be safely ruled out. We are therefore left with the alternative mechanism of picosecond-scale conformation rearrangement suggested by Hintschiche et al.<sup>28</sup> As the contour length (ca. 200 nm) of PFO studied here is much longer than its persistent length, one may argue that the polymer chain tends to coil into a 3-D structure, where energy migration could possibly proceed through intersegmental contacts.<sup>36</sup> This, however, is unlikely to have occurred in view of the high dilution in a good solvent (toluene) and, more importantly, the observed similarity between spectral dynamics of PFO and the oligomers. Furthermore, the conformation relaxation has been consistently observed via time-resolved photoluminescence by changing solvent viscosity at various temperatures. Based on these results, excited-state conformation

rearrangement is considered the prime cause of the spectral red-shift of PFO with increasing delay time. In fact, phenylene oscillation has indeed been identified in the meV range and correspondingly the picosecond time scale.<sup>37</sup>

**Photoacoustic Calorimetry.** To verify the proposed mechanism of torsional motion (and hence energy dissipation) in the excited state, photoacoustic calorimetry (PAC) and photothermal beam deflection (PBD) were adopted as independent routes for quantitative assessments.<sup>38,39</sup> Figure 3a shows normalized PAC traces for 2-hydroxybenzophenone (HBP, as the referencing standard), PFO, and oligofluorenes in toluene. The PAC amplitude (normalized with respect to HBP) is determined as 0.20 (±0.02) for both TSBF and F3, 0.54 for F5, 0.63 for F7, and 0.73 for PFO, increasing clearly with chain length.

As PAC monitors the induced pressure in a liquid sample upon pulsed laser excitation, the PAC amplitude contains contributions from heat relaxation and volume change. In terms of heat relaxation, the PAC amplitude is proportional to the total yield of nonradiative decay paths, including intersystem crossing and internal conversion.<sup>40</sup> For TSBF, it has been reported that the PAC amplitude (0.20, normalized with respect to HBP) is mainly contributed by internal conversion ( $\phi_{IC} = 0.09$ ) and intersystem crossing ( $\phi_T = 0.06$ ), whereas the contribution from volume change is negligible.<sup>41,42</sup> These fluorescence quantum yields ( $\phi$ ) of materials were measured at various concentrations by fluorescence spectrometer. Figure 3b shows the plot of integrated fluorescence intensity vs absorbance (varied by changing the solution concentration within the limit of 0.1 or less in optical density). The slope  $S$  for each sample is proportional to  $\phi$ , which follows the relation  $\phi_x = \phi_s (S_x/S_s)(n_x/n_s)^2$  where  $n$  represents the refractive index of solvent adopted for each measurement while subscripts  $s$  and  $x$  denote the standard and the sample, respectively.<sup>43</sup> Using TSBF as the reference ( $\phi_{TSBF} = 0.85$ ),<sup>41</sup> the fluorescence quantum yields of all samples have been calculated. The fluorescence quantum yield of F3  $\phi_{F3}$  is 0.85, the others are of the similar values of 0.79. The  $\phi_{PFO}$  of 0.79 obtained here is identical to that previously reported.<sup>44</sup> The intersystem crossing of F3 is assumed to be 6% since the photophysics of F3 is similar to that of TSBF. Due to the similarity in photophysical behavior, intersystem crossing yields of F5 and F7 are assumed to be similar to that (4%)<sup>45</sup> of PFO. Note that the triplet state level used here refers to the result from time-resolved photoluminescence and excited-state absorption measurements.<sup>46</sup> Under these conditions, there appears little volume change for F3, as  $\phi_{3F} = 0.85 (= \phi_{TSBF})$  and the PAC amplitude overlaps with that of TSBF.

For other oligomers and PFO, however, PAC amplitudes indicate significant volume changes. In the case of PFO ( $\phi_{PFO} = 0.79$ ),<sup>44</sup> the contribution from heat relaxation is expected to 0.29, which is less than 1/3 of the experimentally observed signal jump of 0.73. This signifies a major contribution from the volume change to the PAC signal of PFO. Solutions of PFO at various concentrations (to give optical densities ranging from 0.08 to 0.6) were subsequently examined, from which the volume change was found to be concentration-independent and hence originated from intrachromophore motion rather than interchromophore interactions. Fluorescence quantum efficiencies of F5 and F7 were the same that of PFO but the corresponding PAC amplitudes were comparatively lower. This, combined with the observation of negligible volume changes in the case of TSBF and F3, signify increasing volume change with the number of repeat units beyond 3. The observed chain length dependence is consistent with the proposed torsion of fluorene units.

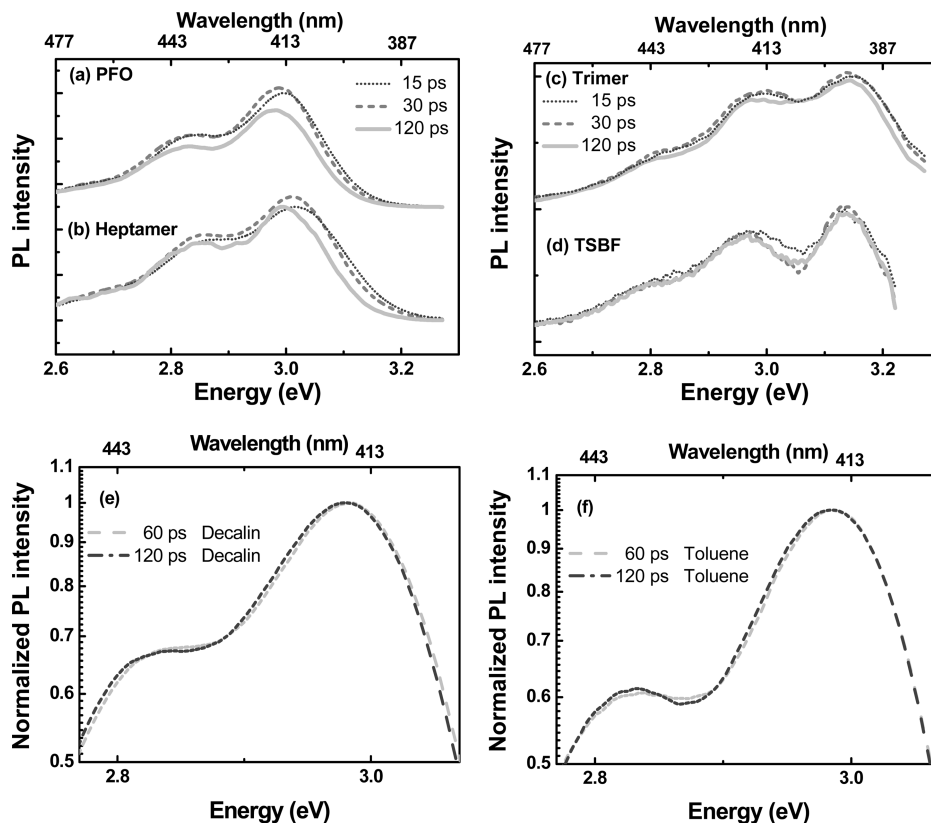


**Figure 2.** Unnormalized TRPL spectra of (a) PFO, (b) F7, (c) F3, and (d) TSBF in toluene. The photoluminescence intensities have been normalized to the spectra at 15 ps (dotted lines) respectively. Lines are the averaged results from time spans ( $\pm 10$  ps) centered at 15, 30, and 120 ps. Normalized TRPL spectra of (e) PFO in decalin (2.4 cP) and (f) PFO in toluene (0.6 cP) reveal some slight spectral shift in the former case but nearly coinciding spectra in the latter, indicating slightly longer lifetime in the more viscous environment.

Assuming that each absorbed photon of energy  $h\nu$  results in one exciton in the dilute solution, the PAC amplitude  $S(t)$  normalized with respect to the reference response  $R(t)$  may be related to the photoinduced volume change  $\Delta V$  and the nonradiative heat generation  $Q(t) \approx h(\nu - \nu_F) + h\nu_F\phi_{IC} + h(\nu_F - \nu_F)\phi_T$  (in which triplet state relaxation is assumed ineffective in the  $\mu$ s-time scale) according to<sup>47</sup>

$$S(t)/R(t) = Q(t)/h\nu + \rho C_p \Delta V(t)/\beta h\nu \quad (1)$$

where  $\rho = 0.867 \text{ g mL}^{-1}$ ,  $C_p = 1.14 \text{ J g}^{-1} \text{ K}^{-1}$ , and  $\beta = 1.09 \times 10^{-3} \text{ K}^{-1}$  are respectively the density, the heat capacity, and the volumetric thermal expansion coefficient of the solvent (toluene). As stated earlier in qualitative terms, the calculated volume changes for TSBF and F3 are  $(\Delta V_{\text{TSBF}})_{\text{PAC}} \approx (\Delta V_{\text{F3}})_{\text{PAC}} \approx 0$  ( $\pm 0.007$  based on noise range). For higher oligomers and PFO, we have  $(\Delta V_{\text{F5}})_{\text{PAC}} = 0.153 \text{ nm}^3/\text{exciton}$ ,  $(\Delta V_{\text{F7}})_{\text{PAC}} = 0.203 \text{ nm}^3/\text{exciton}$ , and  $(\Delta V_{\text{PFO}})_{\text{PAC}} = 0.263 \text{ nm}^3/\text{exciton}$ .

**Photothermal Beam Deflection.** In support of PAC observations, corresponding PBD traces are given in Figure 3c. Normalized amplitudes are 0.23 (TSBF and F3), 0.57 (F5), 0.68 (F7), and 0.79 (PFO) with respect to HBP, mildly but consistently higher than the PAC counterparts. We attribute the “extra” thermal effects to nonradiative triplet-state decay that becomes effective in this case of 30–300  $\mu$ s time span. Hence volume changes were calculated via eq 1 using  $Q(t) \approx h(\nu - \nu_F) + h\nu_F(\phi_{IC} + \phi_T)$  (with the inclusion of nonradiative triplet-state relaxation), yielding  $(\Delta V_{\text{TSBF}})_{\text{PBD}} \approx (\Delta V_{\text{F3}})_{\text{PBD}} \approx 0$  ( $\pm 0.007$ )  $\text{nm}^3/\text{exciton}$ ,  $(\Delta V_{\text{F5}})_{\text{PBD}} = 0.156 \text{ nm}^3/\text{exciton}$ ,  $(\Delta V_{\text{F7}})_{\text{PBD}} = 0.220 \text{ nm}^3/\text{exciton}$ , and  $(\Delta V_{\text{PFO}})_{\text{PBD}} = 0.281 \text{ nm}^3/\text{exciton}$ . As these are comparable to the PAC results, averaged values, i.e.,  $\Delta V_{\text{F5}} =$

$0.155 (\pm 0.010) \text{ nm}^3/\text{exciton}$ ,  $\Delta V_{\text{F7}} = 0.212 (\pm 0.011) \text{ nm}^3/\text{exciton}$ , and  $\Delta V_{\text{PFO}} = 0.272 (\pm 0.013) \text{ nm}^3/\text{exciton}$ , are used for further discussion below.

**Volume Exclusion.** With an effective time window of 3–300  $\mu$ s, PBD measurements provide independent and complementary confirmation of PAC results of  $\mu$ s time span. The quantitative agreement between results of the two techniques reaffirm the proposed “volume change” occurring within 20 ns of photoexcitation. The physical meaning of the molecular volume change, however, deserves further discussion. Results of quantum mechanical calculations<sup>48</sup> give the molecular volume (defined as the volume inside the contour of electron density greater than  $0.001 r_B^{-3}$ ) of a fluorene unit as  $0.210 \text{ nm}^3$  in the ground state ( $S_0$ ), which increases to  $0.225 \text{ nm}^3$  for the first excited state ( $S_1$ ). This corresponds to a volume increase of  $0.044 \text{ nm}^3/\text{molecule}$  of F3, which is small but should have been detectable via PAC or PBD. As molecular volume in the liquid state is typically<sup>49</sup> ca. 12% greater than that in the close-packed crystalline state due to random thermal motions, it is conceivable that this 7% molecular volume change is easily overshadowed by the thermally induced density fluctuations. Hence the straightforward change in hardcore volume upon excitation is unlikely to contribute to PAC- or PBD-observed volume changes. This leads naturally to the consideration of extra volume exclusion due to torsional motion of the fluorene units to account for the experimentally determined volume increase.

The fluorene backbone may be modeled as a sequence of “monomeric boards”, each with length  $l = 0.83 \text{ nm}$ , width  $2w = 0.40 \text{ nm}$ , and thickness  $2t = 0.34 \text{ nm}$  and hence occupying  $0.11 \text{ nm}^3$  in hard-core volume; the side chains (which constitute the rest half of the molecular volume) are assumed flexible



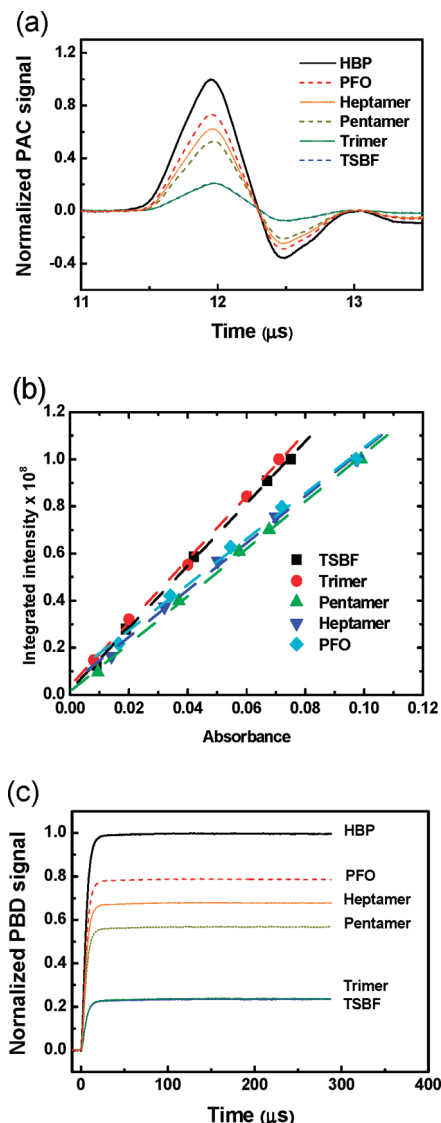


**Figure 3.** Normalized (a) PAC and (c) PBD signals of the reference compound HBP, PFO, heptamer (F7), pentamer (F5), trimer (F3), and TSBF in toluene solutions irradiated at 355 nm. (b) Linear plots of the integrated fluorescence intensity vs absorbance (adjusted by changing solution concentration within the limit of 0.1 or less in optical density). Using TSBS as the standard, the fluorescence quantum yields have been calculated as 0.85 for F3 and 0.79 for others from the slope of the linear fit.

enough to be dragged through the medium without much volume requirement. Upon photoexcitation, one exciton is formed over the effective conjugation length. The volume needed to allow for oscillation of backbone rings would correspond to the part of  $\Delta V$  unaccounted for by excited-state hard-core volume expansion. A simple geometrical analysis gives the extra volume swept by a fluorene unit rotating up to an angle of  $\theta$  as  $\Delta V \approx l(w^2 + t^2) [1 - \tan^2(\theta/2)] \sin \theta \approx l(w^2 + t^2) \sin \theta$  for moderately small  $\theta$ . Taking F5 as an example, relative to the first monomer unit, the others are allowed to rotate by  $\theta$ . The excluded volume per exciton may then be estimated as  $\Delta V_{F5} = 4 \times 0.83 \times 0.069 \sin \theta$  and thus  $\theta = 43^\circ (\pm 3^\circ)$ . For F7, the rotating angle  $\theta$  was estimated as  $\theta = 38^\circ (\pm 2^\circ)$ . The effective conjugation length of PFO was reported as 8 nm,<sup>22,26</sup> which corresponds to ca. 9 repeat units and is consistent to our notion of slightly longer than the heptamer. Using this effective conjugation length, the rotating angle  $\theta$  may be similarly estimated as  $\theta = 37^\circ (\pm 2^\circ)$ . It is therefore concluded that there exist excited state ring torsion

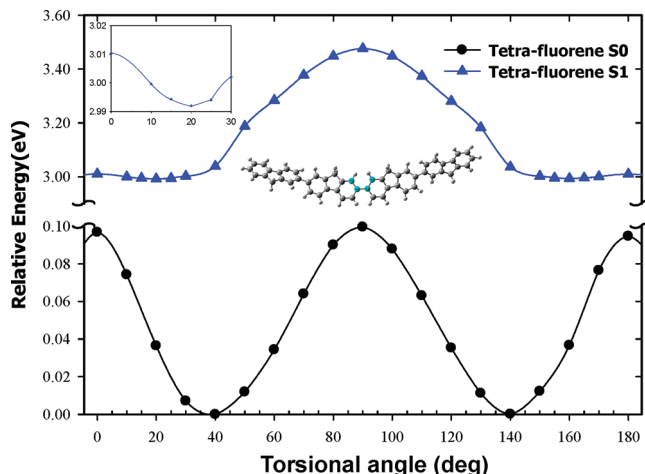


**Figure 4.** Potential curves of tetrafluorene with respect to torsion of the central fluorene-fluorene link. Note that symmetry considerations dictate that the opposite torsion gives the same potential curves. The minimal energy of ground state ( $S_0$ ) is at torsion angles  $\pm 40^\circ$  and  $\pm 140^\circ$ . The minimal energy of the first excited singlet state ( $S_1$ ) state is at torsion angles  $\pm 20^\circ$  and  $\pm 160^\circ$ . The  $S_0$  molecular structure is optimized by HF/6-31G(d) and then the energy is calculated on the B3LYP/6-31+G(d) level; the  $S_1$  molecular structure is optimized via the CIS/6-31G(d) method. The  $S_1$  energy is the sum of  $S_0$  energy (based on the CIS-optimized  $S_1$  structure) calculated on the B3LYP/6-31+G(d) level and the excitation energy computed via the TD-B3LYP/6-311G(d) method. These are all well tested and routinely adopted methods appropriate for demonstrating at least semiquantitatively the general features of potential terrains of interest here.<sup>53</sup>

by ca.  $40^\circ$  in PFO and long oligomers. The absence of such torsional motion in TSBF might be attributed to the rigid and bulky spiro-fluorene substitution. Similar ring oscillation in the case of F3 would expectedly give a volume exclusion of  $\Delta V_{F3} = 2 \times 0.83 \times 0.069 \sin 40^\circ = 0.07 \text{ nm}^3$ . Adding to the hard-core volume change, this implies an effective volume expansion by 11%, which is still overshadowed by random density fluctuations.

**Torsional Potentials.** Further insights may be obtained by results of quantum mechanical calculations. For demonstrative purposes, Figure 4 gives potential curves for torsion around the central link in the ground state ( $S_0$ ) and the first excited state ( $S_1$ ) of tetrafluorene in the absence of alkyl side chains (which contribute little to backbone conjugation and hence play insignificant roles in the discussion of excited state dynamics). The potential maps are essentially symmetric, with energy minima located at torsional angles  $\tau = \pm 40^\circ$  or  $\pm 140^\circ$  in the  $S_0$  state, in general agreement with previous reports.<sup>50–52</sup> For the  $S_1$  state, the energy minima correspond to  $\tau = \pm 20^\circ$  or  $\pm 160^\circ$ , with a steep torsion barrier (ca. 0.5 eV) around  $\tau = \pm 90^\circ$  and very low (0.02 eV) barriers centering around  $\tau = 0^\circ$  or  $\pm 180^\circ$ . The shift in the location of energy minimum suggests torsion from say,  $\tau = \pm 40^\circ$  to  $\pm 20^\circ$ , i.e., torsion amplitudes of  $20^\circ$  to  $60^\circ$  in view of the flat potential terrain around coplanarity. This in fact agrees well with the experimentally derived torsion amplitude of ca.  $40^\circ$ , as PAC/PBD results represent the bulk average.

## Concluding Remarks

In summary, we have studied the excited-state relaxation of oligofluorenes and PFO by photoluminescence and an ultrafast structural change within 30 ps. As the result, the relaxation is found to be associated with the photoinduced conformational changes. Photoinduced torsional motion with average amplitude

of ca. 40° was determined via PAC and PBD measurements, which agreed well with results of quantum mechanical calculations. Analytical methods developed in this work, allowing access to quantitative information on excited-state conformation changes, should also be applicable to biomolecular studies. We note nevertheless that a more sophisticated method, time-resolved liquid-phase X-ray diffraction, has recently been developed for the study of an 8-atom molecule with 1 pm spatial and 100 ps time resolution.<sup>54</sup>

**Acknowledgment.** Financial support from the National Science Council under contract number NSC96-2752-E-007-007-PAE is gratefully acknowledged. Thanks are also due to the National Center for High-performance Computing for computer time and facilities. We take this opportunity to sadly announce our loss of beloved advisor/colleague Professor Wun-Shain Fann on September 26, 2008.

## References and Notes

- (1) Kukura, P.; McCamant, D. W.; Yoon, S.; Wandschneider, D. B.; Mathies, R. A. *Science* **2005**, *310*, 1006.
- (2) Zhu, L.; Sage, J. T.; Champion, P. M. *Science* **1994**, *266*, 629.
- (3) Austin, R. H.; Xie, A.; van der Meer, L.; Redlich, B.; Lindgard, P. A.; Frauenfelder, H.; Fu, D. *Phys. Rev. Lett.* **2005**, *94*, 128101.
- (4) Dias, F. B.; Pollock, S.; Hedley, G.; Palsson, L. O.; Monkman, A.; Perepichka, I. I.; Perepichka, I. F.; Tavasli, M.; Bryce, M. R. *J. Phys. Chem. B* **2006**, *110*, 19329.
- (5) Chang, C. W.; Lu, Y. C.; Wang, T. T.; Diau, E. W. *J. Am. Chem. Soc.* **2004**, *126*, 10109.
- (6) Hultell, M.; Stafstrom, S. *Phys. Rev. B* **2007**, *75*, 104304.
- (7) Elbayoum, M. A.; Halim, F. M. A. *J. Chem. Phys.* **1968**, *48*, 2536.
- (8) Brunner, K.; Tortschanoff, A.; Warmuth, C.; Bassler, H.; Kauffmann, H. F. *J. Phys. Chem. B* **2000**, *104*, 3781.
- (9) Karabunarliev, S.; Bittner, E. R.; Baumgarten, M. *J. Chem. Phys.* **2001**, *114*, 5863.
- (10) Yaliraki, S. N.; Silbey, R. J. *J. Chem. Phys.* **1996**, *104*, 1245.
- (11) Gee, R. H.; Boyd, R. H. *J. Chem. Phys.* **1994**, *101*, 8028.
- (12) Tretiak, S.; Saxena, A.; Martin, R. L.; Bishop, A. R. *Phys. Rev. Lett.* **2002**, *89*, 097402.
- (13) Wong, K. S.; Wang, H.; Lanzani, G. *Chem. Phys. Lett.* **1998**, *288*, 59.
- (14) Lanzani, G.; Nisoli, M.; Magni, V.; Desilvestri, S.; Barbarella, G.; Zambianchi, M.; Tubino, R. *Phys. Rev. B* **1995**, *51*, 13770.
- (15) Barbara, P. F.; Rand, S. D.; Rentzepis, P. M. *J. Am. Chem. Soc.* **1981**, *103*, 2156.
- (16) Hunt, N. T.; Meech, S. R. *Chem. Phys. Lett.* **2004**, *400*, 368.
- (17) Zhang, J. Z.; Kreger, M. A.; Hu, Q. S.; Vitharana, D.; Pu, L.; Brock, P. J.; Scott, J. C. *J. Chem. Phys.* **1997**, *106*, 3710.
- (18) Westenhoff, S.; Beenken, W. J. D.; Friend, R. H.; Greenham, N. C.; Yartsev, A.; Sundstrom, V. *Phys. Rev. Lett.* **2006**, *97*, 166804.
- (19) Di Paolo, R. E.; de Melo, J. S.; Pina, J.; Burrows, H. D.; Morgado, J.; Macanita, A. L. *ChemPhysChem* **2007**, *8*, 2657.
- (20) Song, A.; Liang, W. Z.; Zhao, Y.; Yang, J. L. *Appl. Phys. Lett.* **2006**, *89*, 071917.
- (21) Monkman, A. P.; Burrows, H. D.; Hartwell, L. J.; Horsburgh, L. E.; Hamblett, I.; Navaratnam, S. *Phys. Rev. Lett.* **2001**, *86*, 1358.
- (22) Cadby, A. J.; Lane, P. A.; Mellor, H.; Martin, S. J.; Grell, M.; Giebel, C.; Bradley, D. D. C. *Phys. Rev. B* **2000**, *62*, 15604.
- (23) Chen, S. H.; Su, A. C. S.; C. H. *Macromolecules* **2005**, *38*, 379.
- (24) Monkman, A.; Rothe, C.; King, S.; Dias, F. *Adv. Polym. Sci.* **2008**, *212*, 187.
- (25) Chunwaschirasiri, W.; Tanto, B.; Huber, D. L.; Winokur, M. J. *Phys. Rev. Lett.* **2005**, *94*, 107402.
- (26) Dias, F. B.; Macanita, A. L.; de Melo, J. S.; Burrows, H. D.; Güntner, R.; Scherf, U.; Monkman, A. P. *J. Chem. Phys.* **2003**, *118*, 7119.
- (27) Vaughan, H. L.; Dias, F. B.; Monkman, A. P. *J. Chem. Phys.* **2005**, *122*, 014902.
- (28) Hintschich, S. I.; Dias, F. B.; Monkman, A. P. *Phys. Rev. B* **2006**, *74*, 045210.
- (29) Ridley, C.; Stern, A. C.; Green, T.; DeVane, R.; Space, B.; Mikosovska, J.; Larsen, R. W. *Chem. Phys. Lett.* **2006**, *418*, 137.
- (30) Chang, R.; Hsu, J. H.; Fann, W. S.; Liang, K. K.; Chiang, C. H.; Hayashi, M.; Yu, J.; Lin, S. H.; Chang, E. C.; Chuang, K. R.; Chen, S. A. *Chem. Phys. Lett.* **2000**, *317*, 142.
- (31) Jo, J. H.; Chi, C. Y.; Hoger, S.; Wegner, G.; Yoon, D. Y. *Chem.—Eur. J.* **2004**, *10*, 2681.
- (32) Rissler, J. *Chem. Phys. Lett.* **2004**, *395*, 92.
- (33) Arif, M.; Volz, C.; Guha, S. *Phys. Rev. Lett.* **2006**, *96*, 025503.
- (34) Chang, M. H.; Hoffmann, M.; Anderson, H. L.; Herz, L. M. *J. Am. Chem. Soc.* **2008**, *130*, 10171.
- (35) Fytas, G.; Nothofer, H. G.; Scherf, U.; Vlassopoulos, D.; Meier, G. *Macromolecules* **2002**, *35*, 481.
- (36) Beljonne, D.; Pourtois, G.; Silva, C.; Hennebicq, E.; Herz, L. M.; Friend, R. H.; Scholes, G. D.; Setayesh, S.; Mullen, K.; Bredas, J. L. *Proc. Natl. Acad. Sci.* **2002**, *99*, 10982.
- (37) Quintana, I.; Arbe, A.; Colmenero, J.; Frick, B. *Macromolecules* **2005**, *38*, 3999.
- (38) dos Santos, R. M. B.; Lagoa, A. L. C.; Simoes, J. A. M. *J. Chem. Thermodyn.* **1999**, *31*, 1483.
- (39) Michler, I.; Braslavsky, S. E. *Photochem. Photobiol.* **2001**, *74*, 624.
- (40) Huang, Y. F.; Chen, H. L.; Ting, J. W.; Liao, C. S.; Larsen, R. W.; Fann, W. J. *Phys. Chem. B* **2004**, *108*, 9619.
- (41) Wong, K. T.; Hwu, T. Y.; Balaiah, A.; Chao, T. C.; Fang, F. C.; Lee, C. T.; Peng, Y. C. *Org. Lett.* **2006**, *8*, 1415.
- (42) Chen, H. L.; Huang, Y. F.; Hsu, C. P.; Lim, T. S.; Kuo, L. C.; Leung, M. K.; Chao, T. C.; Wong, K. T.; Chen, S. A.; Fann, W. J. *Phys. Chem. A* **2007**, *111*, 9424.
- (43) Williams, A. T. R.; Winfield, S. A.; Miller, J. N. *Analyst* **1983**, *108*, 1067.
- (44) Burrows, H. D.; de Melo, J. S.; Serpa, C.; Arnaut, L. G.; Monkman, A. P.; Hamblett, I.; Navaratnam, S. *J. Chem. Phys.* **2001**, *115*, 9601.
- (45) King, S. M.; Matheson, R.; Dias, F. B.; Monkman, A. P. *J. Phys. Chem. B* **2008**, *112*, 8010.
- (46) Wasserberg, D.; Dudek, S. P.; Meskers, S. C. J.; Janssen, R. A. J. *Chem. Phys. Lett.* **2005**, *411*, 273.
- (47) Barslavsky, S. E.; Heibel, G. E. *Chem. Rev.* **1992**, *92*, 1381.
- (48) Chen, P. H. M.S. Thesis, Department of Chemical Engineering; National Tsing Hua University: Hsinchu, 2008.
- (49) Van Krevelen, D. W. *Properties of Polymers*, 3rd ed.; Elsevier: Amsterdam, 1997; Chapter 4.
- (50) Volz, C.; Arif, M.; Guha, S. *J. Chem. Phys.* **2007**, *126*, 064905.
- (51) Ignacio Franco, S. T. *J. Am. Chem. Soc.* **2004**, *126*, 12130.
- (52) Tanto, B.; Guha, S.; Martin, C. M.; Scherf, U.; Winokur, M. J. *Macromolecules* **2004**, *37*, 9438.
- (53) Levine, I. N. *Quantum Chemistry*, 5th ed.; Prentice Hall: Upper Saddle River, NJ, 2000; Chapter 17.
- (54) Ihee, H.; Lorenc, M.; Kim, T. K.; Kong, Q. Y.; Cammarata, M.; Lee, J. H.; Bratos, S.; Wulff, M. *Science* **2005**, *309*, 1223.

JP901556V